Journal of Alloys and Compounds 510 (2012) L1–L4

Contents lists available at SciVerse ScienceDirect

Journal of Alloys and Compounds

journal homepage: www.elsevier.com/locate/jallcom

Letter

# First-principles study of pressure-induced magnetic transition in siderite $FeCO_3$

Xing Ming[a,b], Xiao-Lan Wang[a], Fei Du[b,c], Jian-Wu Yin[a], Chun-Zhong Wang[b], Gang Chen[b,*]

[a] College of Physical Science and Technology, Huanggang Normal University, Huanggang 438000, PR China
[b] College of Physics/State Key Laboratory of Superhard Materials, Jilin University, Changchun 130012, PR China
[c] Institute for Solid State Physics, University of Tokyo, 5-1-5, Kashiwanoha, Kashiwa, Chiba, 277-8581, Japan

ARTICLE INFO

*Article history:*
Received 11 June 2011
Received in revised form 22 August 2011
Accepted 25 August 2011
Available online 5 September 2011

*Keywords:*
$FeCO_3$
Magnetic transition
First-principles calculations
High pressure

ABSTRACT

The crystal structure, electronic configuration, spin state and electronic structure of siderite $FeCO_3$ under pressure have been studied by first-principles calculations in the framework of density functional theory (DFT). The real antiferromagnetic (AFM) spin ordering state has been considered and the hydrostatic pressure condition is simulated. The calculated geometric structural data (unit-cell volume $V$, lattice constant $a$, cell angle $\alpha$ and atomic internal coordinate $u$) of $FeCO_3$ at ambient condition in good agreement with available data from the literature. $FeCO_3$ transforms from high spin (HS) AFM state to low spin (LS) nonmagnetic (NM) state between 40 and 50 GPa, concomitant with a volume collapse of 11%. The unit cell volume $V_0$, bulk moduli $B_0$, and its pressure derivative $B'_0$ of the HS and LS state are fit with a 3rd-order Birch–Murnaghan equation of state, which consist well with available experimental results. The insulating nature of $FeCO_3$ is remained after the magnetic transition. The 3d electrons of $Fe^{2+}$ ions for the LS NM state are more localized than those of the HS AFM state, which leading to the magnetic transition.


## 1. Introduction

Siderite ($FeCO_3$) is a ferrous mineral widespread on earth, which is a valuable iron mineral because it contains 48% iron and does not contain sulfur or phosphorus. Siderite ($FeCO_3$) is an isostructural mineral of calcite ($CaCO_3$) and magnesite ($MgCO_3$). The detailed crystalline structure of siderite ($FeCO_3$) has been studied by Wyckoff [1], Cowley [2], and Rao et al. [3], which belongs to the hexagonal system with rhombohedral shape. The space group of $FeCO_3$ is $R\bar{3}C$, and the crystallographic unit cell consists of two molecular formula units with two Fe atoms. As shown in Fig. 1, Fe, C and O atoms are located at the cell origin (0 0 0), the position of (0 0 1/4) and ($u$ 0 1/4) in a hexagonal setting, respectively, where $u$ is an atomic internal structural parameter. The C atoms lie in the plane surrounded by its three neighboring O atoms forming $CO_3$ plane perpendicular to the $c$ axis. Each Fe atom is surrounded by six O atoms belonging to six different $CO_3$ groups, forming a $FeO_6$ octahedron.

$FeCO_3$ is an insulating compound but the band gap is not clear. Generally, $FeCO_3$ is assigned to be an ionic crystal, where $Fe^{2+}$ ions assume with an electronic configuration of (Ar) $3d^6 4s^0$. So the $Fe^{2+}$ ions can adopt a high spin (HS, $S=2$) or low spin (LS, $S=0$) state. Magnetic susceptibility and neutron-diffraction experiments have indicated that $FeCO_3$ was an antiferromagnetic (AFM) compound with a low Néel temperature of 38 K [4–8]. All the magnetic moments ($Fe^{2+}$ ion) are ferromagnetically (FM) coupled inside a (0 0 0 1) Fe plane, whereas neighboring planes along the $c$ axis are antiferromagnetically coupled. Siderite shows the metamagnetic transition from the antiferromagnetism towards ferromagnetism [4].

Though a number of works have been reported on compression behaviors of calcite and magnesite, relatively few experiments and theoretical works have been reported for the properties of siderite under high pressure. Zhang et al. reported compression data of $FeCO_3$ up to 8.9 GPa and 1073 K [9]. Santillán and Williams found that the crystal structure of $FeCO_3$ is stable up to 50 GPa at room temperature by infrared spectroscopy and high-pressure X-ray diffraction experiments [10]. Mattila et al. reported a pressure-induced spin transition from HS to LS nonmagnetic (NM) state for $Fe^{2+}$ ion in $FeCO_3$ by X-ray emission spectroscopy (XES) around 50 GPa at room temperature [11]. Nagai et al. reported synchrotron X-ray diffraction patterns of $FeCO_3$-siderite after or in situ laser heating at high pressures up to 66 GPa [12]. The calculated cell volumes show an abrupt decrease (about 6.5%) between 47 and 50 GPa at room temperature, which is possibly due to a pressure-induced spin transition of $Fe^{2+}$ ion. Lavina et al. presented detailed observations of the pressure-induced spin-pairing transition by means of single-crystal X-ray diffraction [13]. The spin pairing occurs over a narrow pressure range of 44–45 GPa, concomitant with a shrinkage of the octahedral bond distance by 4%, and a volume collapse of 10%. They also reported that the spin-pairing phenomenon shows hysteresis in decompression.

* Corresponding author.
*E-mail addresses:* mingxing06@mails.jlu.edu.cn (X. Ming), gchen@jlu.edu.cn (G. Chen).

0925-8388/$ – see front matter © 2011 Elsevier B.V. All rights reserved.
doi:10.1016/j.jallcom.2011.08.079

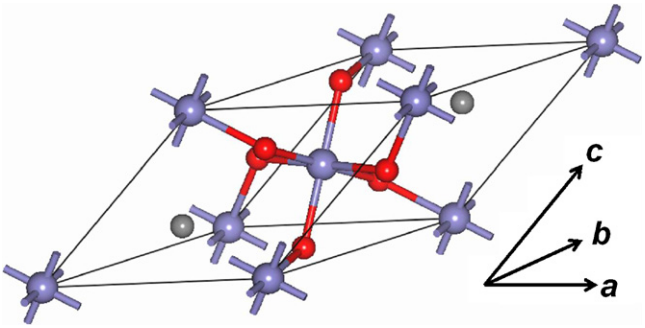


**Fig. 1.** Primitive unit cell of $FeCO_3$ consisting of two formula units. Blue, gray, and red spheres represent Fe, C, and O atoms, respectively.

Because the surface of pure siderite is quickly oxidized under atmospheric conditions, hence theoretical investigations could help to better understand the crystal structure, electronic structure, magnetic properties of siderite. Sherman presented theoretical calculations of the crystal structure parameters, Mulliken effective charges, spin populations, electronic structure and the O *K*-edge absorption spectra of $FeCO_3$, using periodic density functional theory (DFT) with generalized gradient approximation (GGA) and B3LYP hybrid functionals [14]. Badaut et al. studied the structural, electronic, and elastic properties of $FeCO_3$ at ambient conditions by DFT calculations [15]. The pressure-induced magnetic phase transition, electronic structure of $FeCO_3$, as well as geometrical structure have been studied by Shi et al. using first-principles calculations with GGA [16]. They observed a pressure-induced magnetic transition (HS to LS) at pressures of 15 and 28 GPa by GGA and GGA + U calculations, which are underestimated with respect to the experimental value. They obtained an insulating band gap with both standard GGA and GGA + U schemes and reported completely empty iron 3d minority-spin states for the electronic structure, corresponding to highly impossible $Fe^{3+}$ and $CO_3^{3-}$ formal charge states.

This work aims to explore the properties of siderite $FeCO_3$ under high pressure by first-principles calculations within plane wave pseudo-potential method. The real AFM spin ordering state of $FeCO_3$ has been considered under hydrostatic pressure condition. $FeCO_3$ transforms from HS AFM state to LS NM state between 40 and 50 GPa, concomitant with a volume collapse of 11%. The 3d electrons of $Fe^{2+}$ ions for the LS NM state are more localized relative to those of the HS AFM state. Present theoretical calculated results consist well with experimental data.

## 2. Computational method

The *ab initio* calculations performed in this work were done using the CASTEP code [17] based on DFT with Vanderbilt-type ultrasoft pseudopotentials [18] and a plane-wave expansion of the wave functions. The valence electrons considered in this work are Fe ($3d^6 4s^2$), C ($2s^2\ 2p^2$), and O ($2s^2 2p^4$). The exchange-correlation functional proposed by Perdew, Burke, and Ernzerhof (PBE) [19] was employed to treat the exchange-correlation functional. The electron wave function is expanded by plane wave up to an energy cutoff of 800 eV for all calculations. Requested *k*-point spacing is fixed to 0.04 $Å^{-1}$ in the irreducible Brillouin zone according to the special *k*-points sampling scheme of Monkhorst-Pack method [20].

The initial AFM magnetic structure is built according to the neutron-diffraction experimental data by setting the spin moments of two $Fe^{2+}$ ions antiparallel in the rhombohedral unit-cell [8]. Geometry optimizations are performed to fully relax the atomic internal coordinates and the lattice parameters within the BFGS minimization algorithm [21]. All the structures are relaxed by elaborate geometry optimization under pressure to implement constant-pressure *ab initio* simulations to find its lowest-energy state. The self-convergence thresholds for energy change, maximum force, maximum stress, and maximum displacement between optimization cycles are $5 \times 10^{-6}$ eV/atom, 0.01 eV/Å, 0.02 GPa and $5 \times 10^{-4}$ Å.

**Table 1**
Calculated and experimental structural data (unit-cell volume *V*, lattice constant *a*, cell angle $\alpha$ and atomic internal coordinate *u*) of $FeCO_3$ at ambient condition.

| | | $V$ (Å$^3$) | $a$ (Å) | $\alpha$ (°) | $u$ |
|---|---|---|---|---|---|
| This work | GGA | 98.23 | 5.785 | 48.09 | 0.276 |
| Ref. [16] | GGA | 98.40 | 5.770 | 48.35 | 0.274 |
| Ref. [16] | GGA + U (4 eV) | 99.39 | 5.782 | 48.49 | 0.272 |
| Ref. [16] | GGA + U (5 eV) | 99.46 | 5.786 | 48.46 | 0.272 |
| Ref. [16] | GGA + U (6 eV) | 99.24 | 5.781 | 48.47 | 0.272 |
| Ref. [15] | GGA | 97.446 | 5.768 | 48.10 | – |
| Ref. [14] | GGA | 96.80 | 5.6892 | 49.159 | – |
| Ref. [14] | B3LYP-20%HF | 98.79 | 5.6914 | 49.755 | – |
| Ref. [14] | B3LYP-10%HF | 98.97 | 5.6877 | 49.875 | – |
| Expt. [1] | – | 97.63 | 5.795 | 47.75 | 0.27 |
| Expt. [13] | – | 98.14 | 5.797 | 47.73 | 0.275 |
| Expt. [22] | – | 97.064 | 5.798 | 47.73 | – |

## 3. Results and discussion

The calculated structural parameters of $FeCO_3$ at ambient condition together with other theoretical calculated results and the experimental data are listed in Table 1. Our calculated results are in good agreement with available experimental data and other theoretically calculated results, which confirms the accuracy of our calculations. The calculated spin moment is 3.70 $\mu_B$ per $Fe^{2+}$ ion, which is comparable with the expected value of $3d^6$ electronic configuration (4 $\mu_B$). Present theoretical calculated magnetic moment is in line with calculated results using PBE and B3LYP functional [14], which confirms the experimentally determined HS configuration of the $Fe^{2+}$ ($3d^6$) ion.

The calculated volume dependence of pressure for $FeCO_3$ is plotted in Fig. 2. The unit cell volume decreases abruptly with a volume collapse of about 11% around 40–50 GPa, which consist well with the experimental observed phenomena [11–13]. Present theoretical calculated transition pressure agrees better with experimental results relative to those in Ref. [16]. The abrupt change of the cell volume of $FeCO_3$ is due to a pressure-induced spin transition of $Fe^{2+}$ ion from HS to LS state (will demonstrate latter). By fitting the variation of volume pressure data between 0 and 40 GPa by a 3rd order Birch–Murnaghan equation of state (BM-EOS) [23], we obtained the volume of the equilibrium state ($V_0$ = 98.20 Å$^3$), bulk modulus ($B_0$ = 112 GPa) and pressure derivative of the bulk modulus ($B'_0$ = 3.5) for the HS state $FeCO_3$, which are in good agreement

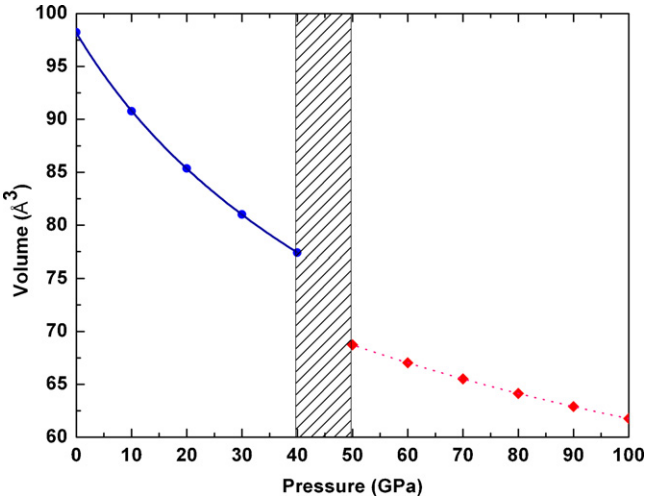


**Fig. 2.** The calculated volume dependence of pressure for $FeCO_3$. A magnetic transition from HS to LS state occurs around 40–50 GPa. The solid and dotted curves represent the best fit to the 3rd order BM-EOS for the HS and LS state of $FeCO_3$, respectively. The shadow region marks the volume collapse of about 11% and magnetic transition from HS to LS state.

**Table 2**
The zero pressure volume $V_0$, bulk modulus $B_0$ and pressure derivative of the bulk modulus $B'_0$ for the HS state $FeCO_3$ from theoretical calculated (Cal.) and experimental (Expt.) results.

| | EOS | $V_0$ (Å$^3$) | $B_0$ | $B'_0$ |
|---|---|---|---|---|
| This work | BM | 98.20 | 112 | 3.5 |
| Cal. [16] | BM | 99.46 | 114 | 4.0 |
| Cal. [15] | BM | 97.27 | 108 | 4.5 |
| Cal. [15] | Vinet | 97.27 | 106 | 4.8 |
| Expt. [13] | BM | 98.14 | 110 | 4.6 |
| Expt. [13] | BM | 98.14 | 117 | 4 |
| Expt. [12] | BM | – | 120 | 4.3 |
| Expt. [9] | BM | 96.95 | 127 | 4.0 |
| Expt. [9] | Vinet | 96.95 | 129 | 3.4 |

with the experimental measured and theoretical calculated values from the literature (Table 2). We also fit the volume pressure data between 50 and 100 GPa to calculated the zero pressure volume ($V_0$ = 82.93 Å$^3$), bulk modulus ($B_0$ = 175 GPa) and the pressure derivative of the bulk modulus ($B'_0$ = 4.4) for the LS state $FeCO_3$. Lavina et al. [24] assigned $B'_0$ = 5.0, using a 3rd order BM-EOS to fit the pressure-volume experimental data of LS $FeCO_3$, obtained a zero pressure volume of 87.67 Å$^3$ and bulk modulus of 148 GPa, respectively. Badaut et al. [15] calculated the unit cell volume (82.864 Å$^3$) of the equilibrium state for the LS NM state of $FeCO_3$ by first-principles calculations, which consist well with the present theoretical fit results. The discrepancy between the theoretical and experimental results can be attributed to the natural siderite used by Lavina et al. [24], whereas ideal $FeCO_3$ crystal structure is adopted in Ref. [15] and this letter.

The variation of the magnetic moment with pressure is presented in Fig. 3. The magnetic moment of HS $FeCO_3$ collapse at 50 GPa, which demonstrating the magnetic transition of $Fe^{2+}$ ($3d^6$) ion from HS to NM LS configurations. The 3d levels split into threefold degenerate $t_{2g}$ ($d_{xy}$,$d_{yz}$,$d_{zx}$) and doubly degenerate $e_g$ $\left(d_{z^2}, d_{x^2-y^2}\right)$ levels in the octahedral crystal field (CF) as shown in the inset of Fig. 3. As a result of the competition among CF splitting, on-site Coulomb correlation effects and intra-atomic Hund's rule exchange coupling, the $Fe^{2+}$ ($3d^6$) ion can adopt three possible electronic configurations, i.e., LS ($t^6{}_{2g}e^0{}_g$, $S$ = 0), intermediate spin (IS) ($t^5{}_{2g}e^1{}_g$, $S$ = 1) and HS ($t^4{}_{2g}e^2{}_g$, $S$ = 2) states. Though these relevant energy scales are important for the spin states of $Fe^{2+}$ ion, only the CF splitting is extraordinary sensitive to pressure [25]. It has been established that the spin state transition is primarily controlled by competition between the CF splitting and the intra-atomic exchange coupling. The intra-atomic exchange coupling favours HS state with a maximum spin multiplicity, whereas the crystal field splitting favours LS state in which the electrons occupy low-energy orbitals only at the expense of increasing the exchange energy [26]. Calculated structural parameters indicate that the spin transition is accompanied by a dramatic decrease of the Fe–O bond length from 1.965 to 1.867 Å (shrinkage by about 5%), which leads to strong hybridization between iron 3d and oxygen 2p bonding states. The CF splitting enhances dramatically under pressure [27,28]. Therefore, system transforms to a LS state when the CF splitting exceeds the Hund's rule exchange energy.

The band structures of $FeCO_3$ at 40 GPa (before spin transition) and 50 GPa (after spin transition) are presented in Fig. 4, where the Fermi level ($E_F$) is set to 0 eV. One prominent characteristic of the band structures is the spin-up and spin-down subbands overlap each other, displaying the AFM ordering of the HS state and NM characteristic of the LS state for $FeCO_3$. The insulating band gap of the HS state has reduced to 0.075 eV due to the well-known bandwidth broadening under pressure. The valence bands extending from −13 to −4 eV are derived from the occupied O 2p states, which are split off from a manifold of Fe 3d bands from −3.5 eV

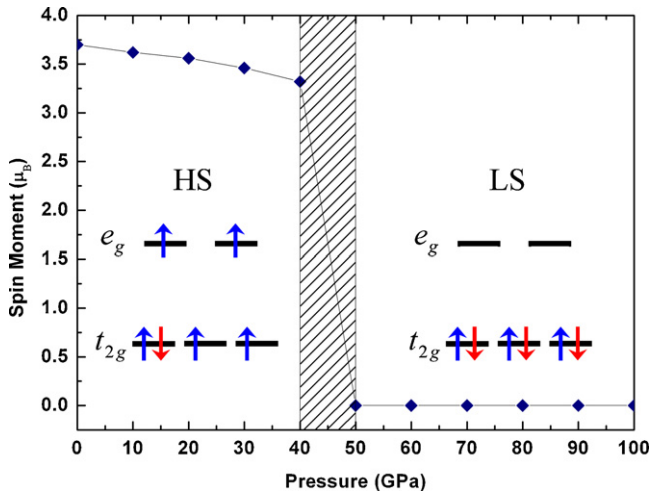


**Fig. 3.** Variation of the spin magnetic moment of $Fe^{2+}$ ($3d^6$) ion with pressure in $FeCO_3$. The shadow region marks the magnetic transition from HS to LS state. The insets are schematic diagrams of the HS and LS spin configurations for the $Fe^{2+}$ ($3d^6$) ions.

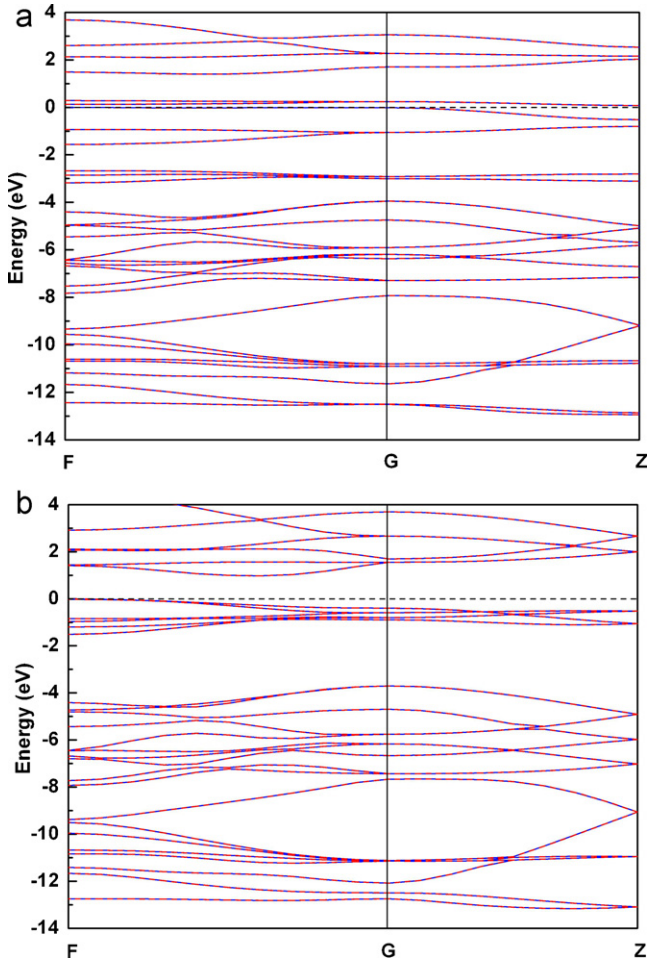


**Fig. 4.** Variation of the electronic structure of $FeCO_3$ from HS AFM to LS NM state: (a) the band structure for the HS state at 40 GPa (before spin transition) and (b) the band structure for the LS state at 50 GPa (after spin transition). The horizontal dashed line at 0 eV is corresponding to the Fermi level ($E_F$). The spin-up/down subbands are plotted with solid/dashed lines, which overlap each other due to the AFM ordering of the HS state and NM characteristic of the LS state.

to $E_F$. The top of the valence band and the bottom of the conduction band are predominantly derived from Fe 3d states strongly localized around $E_F$.

Pressure strongly affects the structural, transport, and magnetic properties of transition metal oxides, which often leading to magnetic collapse, spin state transition and the insulator-metal transition. Spin state is an important issue for many ferri-compounds, which strongly affects or even determines their structural, electric, magnetic, and transport properties. The present DFT electronic structure calculations reveal a spin transition of $Fe^{2+}$ ion with simultaneous volume collapse in $FeCO_3$ under pressure. The spin state of $Fe^{2+}$ ion changes from HS to LS spin configuration under pressure, where the 3d electrons are pairwise compensated and fill in the three $t_{2g}$ orbitals in the NM LS state ($S = 0$). Hence, the ionic radius of the LS state is smaller than the HS state. The different ionic radii of the LS and HS states result in the volume collapse at the spin-state transition similar to the case of $CaFeSi_2O_6$ [27]. Electronic structures indicate $FeCO_3$ remaining the insulating nature after the spin transition, and the band gap of the NM LS state is 0.97 eV, which consist well with the experimental results [13,24]. The essential characteristics of the valence bands for the LS state from −13 to −4 eV are the same as those of the HS state. The remarkable characteristic of the band structures is the Fe 3d bands becoming obvious narrower relative to those of the HS state, indicating a further localization of the Fe 3d electrons, which leading to the HS to LS spin transition.

## 4. Conclusions

The crystal structure, electronic configuration, spin state and electronic structure of siderite $FeCO_3$ under pressure have been studied by first-principles calculations. The calculated ground-state geometric properties such as the equilibrium volume, lattice constants, internal structural parameter, bulk moduli and its pressure derivative, as well as the HS to LS magnetic transition pressure give good agreement with experimental data. $FeCO_3$ transforms from HS AFM state to LS NM state between 40 and 50 GPa, accompanying a volume collapse of 11%. Siderite $FeCO_3$ is insulating before and after the magnetic phase transition. The 3d electrons of $Fe^{2+}$ ions for the LS NM state are more localized relative to those of the HS state, which resulting in the HS to LS spin transition.

## Acknowledgments

This work was sponsored by the National Natural Science Foundation of China (NSFC) under grant no. 11104101 and 11004073, and also partially supported by Scientific and Technologic Research Programs of Hubei Provincial Department of Education under grant no. Q20102901, by Research Fund for the Doctoral Program of Higher Education of China (new teacher) under grant no. 20090061120020 and Open Project of State Key Laboratory of Superhard Materials (Jilin University) under grant no. 201102.

## References

[1] W.G. Wyckoff, Crystal Structure, Interscience, New York, 1948.
[2] E.R. Cowley, Can. J. Phys. 47 (1969) 381.
[3] K.R. Rao, S.F. Trevino, K.W. Logan, J. Chem. Phys. 53 (1970) 4645.
[4] I. Jacobs, J. Appl. Phys. 34 (1963) 1106.
[5] J. Becquerel, J. van den Handel, J. Phys. Radium 10 (1939) 10.
[6] Y.-Y. Zhou, C.-H. Yin, Phys. Rev. B 47 (1993) 5451.
[7] H. Bizette, J. Phys. Radium 12 (1951) 161.
[8] R.A. Alikhanov, Sov. Phys. JETP 9 (1959) 1204.
[9] J. Zhang, I. Martinez, F. Guyot, R. Reeder, Am. Miner. 83 (1998) 280.
[10] J. Santillán, Q. Williams, Phys. Earth Planet. Inter. 143–144 (2004) 291.
[11] A. Mattila, T. Pylkkanen, J.-P. Rueff, S. Huotari, G. Vanko, M. Hanfland, M. Lehtinen, K. Hamalainen, J. Phys.: Condens. Matter 19 (2007) 386206.
[12] T. Nagai, T. Ishido, Y. Seto, D. Nishio-Hamane, N. Sata, K. Fujino, J. Phys.: Conf. Ser. 215 (2010) 012002.
[13] B. Lavina, P. Dera, R.T. Downs, W. Yang, S. Sinogeikin, Y. Meng, G. Shen, D. Schiferl, Phys. Rev. B 82 (2010) 064110.
[14] D.M. Sherman, Am. Miner. 94 (2009) 166.
[15] V. Badaut, P. Zeller, B. Dorado, M.L. Schlegel, Phys. Rev. B 82 (2010) 205121.
[16] H. Shi, W. Luo, B. Johansson, R. Ahuja, Phys. Rev. B 78 (2008) 155119.
[17] S.J. Clark, M.D. Segall, C.J. Pickard, P.J. Hasnip, M.J. Probert, K. Refson, M.C. Payne, Z. Kristallogr. 220 (2005) 567.
[18] D. Vanderbilt, Phys. Rev. B 41 (1990) R7892.
[19] J.P. Perdew, K. Burke, M. Ernzerhof, Phys. Rev. Lett. 77 (1996) 3865; J.P. Perdew, K. Burke, M. Ernzerhof, Phys. Rev. Lett. 78 (1997) 1396(E).
[20] H.J. Monkhorst, J.D. Pack, Phys. Rev. B 13 (1976) 5188.
[21] B.G. Pfrommer, M. Cote, S.G. Louie, M.L. Cohen, J. Comput. Phys. 131 (1997) 133.
[22] H. Effenberger, K. Mereiter, J. Zemann, Z. Kristallogr. 156 (1981) 233.
[23] F.D. Murnaghan, Proc. Natl. Acad. Sci. U.S.A. 30 (1944) 244–247.
[24] B. Lavina, P. Dera, R.T. Downs, V. Prakapenka, M. Rivers, S. Sutton, M. Nicol, Geophys. Res. Lett. 36 (2009) L23306.
[25] A. Trueba, P. Garcia-Fernandez, J.M. Garca-Lastra, J.A. Aramburu, M.T. Barriuso, M. Moreno, J. Phys. Chem. A 115 (2011) 1423.
[26] T. Kawakami, Y. Tsujimoto, H. Kageyama, X.-Q. Chen, C.L. Fu, C. Tassel, A. Kitada, S. Suto, K. Hirama, Y. Sekiya, Y. Makino, T. Okada, T. Yagi, N. Hayashi, K. Yoshimura, S. Nasu, R. Podloucky, M. Takano, Nat. Chem. 1 (2009) 371.
[27] S.V. Streltsov, N.A. Skorikov, Phys. Rev. B 83 (2011) 214407.
[28] J.M. García-Lastra, M. Moreno, M.T. Barriuso, J. Chem. Phys. 128 (2008) 144708.